

## SOIL TEXTURE AND GRANULOMETRY AT THE SURFACE OF MARS

Audouin Dollfus and Marc Deschamps

Observatoire de Paris, Meudon, France

James R. Zimbelman

Center for Earth and Planetary Sciences, National Air and Space Museum  
Smithsonian Institution, Washington, D. C.

The physical behavior of the Martian surface soil has been characterized remotely by both photopolarimetry and radiometry. The degree of linear polarization defines a coefficient  $b$  which is related to the top surface soil texture and is calibrated in terms of grain size, or as a fraction of the area exhibiting uncovered clean rocks. This coefficient  $b$  was recorded with the instrument VPM (Visual Polarimeter Mars) on board Soviet orbiter MARS 5 in 1974. The radiometric thermal inertia coefficient  $I$  is essentially a measurement of the soil compaction, or an effective average particle size in the soil texture, through the few decimeters below the top surface sensed by polarimetry. The instrument IRTM (Infra Red Thermal Mapper) was used on board the Viking spacecraft between 1976 and 1982. The polarimetric scans raked a strip covering two contrasting regions, the dark-hued Mare Erythraeum and the light-hued Thaumasia. Over these wide areas, several smaller typical terrains were characterized by the three parameters  $A$  (albedo),  $b$  (related to top surface grain size) and  $I$  (underlying compaction or block size). The large dark region Erythraeum is characterized everywhere by a uniform polarization response, despite the large geomorphological diversity of the surface. The values of  $A$  and  $b$  indicate a ubiquitous coating or mantling with small dark grains of albedo 12.7%, with a radius of 10 to 20  $\mu\text{m}$ . Thermal inertia coefficient  $I$  indicates that the sub-surface is divided in pieces around 300 to 600  $\mu\text{m}$  in size. A simple model consisting of sand-size particles completely coated with 15  $\mu\text{m}$  black grains is compatible with both measurements. Conversely, the brighter terrain Thaumasia discloses a large variety of soil properties. A typical location with albedo 16.3% has a surface covered with orange grains, probably very dispersed in size, for which the largest grains are 20 to 40  $\mu\text{m}$ . The subsurface is divided into pieces 180-300  $\mu\text{m}$  or smaller, if cemented. On the basis of terrestrial analogs of the Martian soil (Morris et al., 1990), it is surmised that the near-surface soil on the dark areas could be tachylite sand-size grains superficially coated by cohesive black particles of titanomagnetite. The bright orange grains in the Thaumasia-like terrains could be made of the weathered (palagonitized) basalt glass particles of sideromelane, as found in terrestrial analogs (Singer, 1982). Thaumasia is known to be a source area for dust storm production. The observed soil texture provides the large grains needed for saltation to occur, causing the intermixed small grains to be ejected from the surface and carried by wind.

## Introduction

Historically, the nature of the soil surface of Mars was first discovered by optical polarimetry at the telescope [Dollfus, 1958]. The surface was found to be essentially covered by a layer of small grains made of hydrated ferric oxides of limonite, goethite or hematite, indicating a highly oxidized state for the surface [Dollfus and Focas, 1969; Dollfus et al., 1969]. The Viking landers gave in situ confirmation of these results in two areas. The landers documented the presence of boulders, sampled the powdery layers and analyzed the basic physics and mineralogy of the surface material [Mutch et al., 1976a, b, c; Shorthill et al., 1976; Moore et al., 1977; Jakosky and Christensen, 1986a; Moore and Jakosky, 1989]. Through remote analysis from

orbiters, some characterizations of the surface were extended over the whole planet, covering a large variety of terrains. The basic conclusion is that a layer of small grains appears to be ubiquitous, covering the soil almost everywhere over the planetary surface, although with local variations in its properties.

Among the planned projects for future in situ exploration of Mars, rovers will have to move through this layer of small grains, balloon guide-ropes will be trailed across the dust, and penetrometers will go through the dust, leaving small stations at the surface. Sample return missions must include collectors that will extract pieces embedded in this dust layer. Further characterization of the soil properties in its upper layer is needed to support these efforts, as well as to further constrain the likely origin of the materials present within the surface layer.

Copyright 1993 by the American Geophysical Union.

## Soil Surface Characterization Parameters

Paper number 92JE01502.  
0148-0227/93/92JE-01520\$05.00

The present work attempts to characterize the physical behavior of the Martian upper surface in

its first few decimeters on the basis of mutual relationships between three parameters: the linear polarization of the reflected light, the visual albedo, and the thermal inertia.

Polarization parameter  $b$  characterizes the surface texture and grain size at the very top layer of the exposed surface. It is derived from measurements of the degree of linear polarization of the reflected light recorded in 1974 by the photopolarimeter Visual Polarimeter Mars (VPM) on board the Soviet orbiter spacecraft Mars 5 [Ksanfomaliti et al., 1975; Ksanfomaliti and Dollfus, 1976; Dollfus et al., 1977]. The VPMs were cross-calibrated at Meudon Observatory in France and at Space Research Institute of Moscow, IKI. Details of the measurements and initial interpretations of the VPM data are described elsewhere [Dollfus et al., 1983; Dollfus and Deschamps, 1986; Deschamps and Dollfus, 1987]. For the present purpose, only four sequences of VPM measurements were used. They scanned the planet at a wavelength of 592 nm along parallel strips from Thaumasia Fossae ( $-35^\circ$ ,  $85^\circ$ ) to Bosphoros Planum ( $-35^\circ$ ,  $65^\circ$ ) and Mare Erythraeum ( $-25^\circ$ ,  $30^\circ$ ). The exact pointing positions were checked by the photographs such as those reproduced in the Figures 11 to 13, taken simultaneously with the bore-sighted cameras. The footprint resolution was 20 km near periapsis. Atmospheric effects such as hazes, mists, and identified dust clouds were excluded [Santer et al., 1985].

The maximum value of the degree of linear polarization ( $P_{\max}$ ) occurs around a phase angle of  $100^\circ$ . The accuracy in the  $P_{\max}$  determination is around  $\pm 0.2\%$ .  $P_{\max}$  is sensitive to both albedo and soil microtexture over for the first millimeter or less of the top exposed surface. Correction of  $P_{\max}$  by albedo  $A$  produces a polarization parameter  $b$  which is  $b = \log P_{\max} - a \log A$ , in which  $a$  is of known value;  $b$  is related to the surface texture only, as calibrated by laboratory measurements in terms of grain size [Geake and Dollfus, 1986; Dollfus and Deschamps, 1986; Deschamps and Dollfus, 1987]. Parameter  $b$  is derived with an accuracy of  $\pm 0.3\%$ .

Albedo  $A$  discriminates between different types of terrain composition based on the intensity of reflected sunlight.  $A$  is obtained from data reduced to normal incidence and phase angle of  $5^\circ$ , in order to avoid the sharp increase around retro diffusion (opposition effect), which belongs to physical processes other than those under study in the present analysis. The Mars 5 photopolarimeter VPM produced photometric measurements simultaneously with polarimetry for phase angles  $60^\circ$  and  $90^\circ$ . The Viking instruments Infra Red Thermal Mapper IRTM and cameras gave flux measurements which were converted to albedo [Thorpe, 1977; Pleskot and Miner, 1981; Martin, 1981; Christensen, 1988]. Using all of these data, albedo values were derived and modeled for phase angle  $5^\circ$  with an accuracy of around 2% (Dollfus et al., 1986).

Thermal inertia parameter  $I$  relates the thermal conductivity  $K$ , the soil volumetric density, and the specific heat  $C$ , with  $I = (KC)^{1/2}$ . It characterizes essentially the soil compaction in the first few decimeters beneath the surface. Determinations of coefficient  $I$  were obtained from radiometric measurements made by the orbiter Mars 5, simultaneously and along the same ground tracks as for polarimetry [Vdovine et al.,

1980]. The IRTM instrument on board orbiter Viking provided a global mapping of coefficient  $I$  [Kieffer et al., 1977; Palluconi and Kieffer, 1981; Haberle and Jakosky, 1991]. The error in  $I$  does not exceed 0.5%.

The values for the three parameters  $b$ ,  $A$ , and  $I$  considered here are displayed in Figures 1a, 1b and 1c, where they are plotted as a function of the planetary longitude along the four ground tracks of the photopolarimeter VPM, labeled 101, 103, 106, and 109, respectively [see Dollfus et al., 1983].

#### Selected Areas

Several types of terrains were encountered along the tracks extended across the surface by the four adjacent scans. Areas corresponding to distinctive values in one of the three parameters are labeled A to F in Figure 1. Their locations are given in the Figure 2, within the context of the regional albedo features. Each location is more precisely outlined in Figure 3, which also gives the regional contours of the inertia parameter  $I$ . The geomorphologic and tectonic environments of each location are documented in Figures 4 to 6. Area D' was selected as a reference for atmospheric effects because a thin dust veil covered the region [Santer et al., 1985]. The atmospheric feature was detected on the scans is visible on the Mars 5 images taken simultaneously with the scans.

#### Comparison Between the Parameters

Polarimetry (parameter  $b$ ) only penetrates the first few hundreds of microns of the surface layer and characterizes the granulometric properties of the soil at the top surface. Radiometry (parameter  $I$ ) is sensitive to the first few decimeters and characterizes the compaction of the soil below the thin surface sensed by polarimetry. Photometry (parameter  $A$ ) characterizes the absorption of the top surface material and its related composition.

The relationship between polarization parameter  $b$  and albedo  $A$  is presented in the Figure 7. Both parameters describe the uppermost layer of the soil. Values from the selected terrains A to F are circled and labeled. The vertical scale at right gives the grain size derived from the  $b$  values of the scale at left, with the assumption that the surface is made of grains of a uniform size, piled up without cohesion [Geake and Dollfus, 1986]. When there is a distribution in size, the calibration essentially gives the size of those grains which produce the most efficient cross section to the surface, which are the larger grains, but this does not totally exclude the presence of smaller grains. If cohesion between the grains builds up aggregates, flakes, or loose clods, photopolarimetry still characterizes the size of those individual grains which are in contact. When there is a cement between the grains, as in a duricrust texture, the distances between scatterers are not everywhere larger than the wavelength. In this case, polarimetry may derive a size intermediate between the grains and clods.

Another interpretation is to assume a mosaic with a fraction  $f$  of the surface covered with small grains (15  $\mu\text{m}$  in size) of albedo  $A$ , and the remaining area  $(1-f)$  covered by hard, bare, rocky

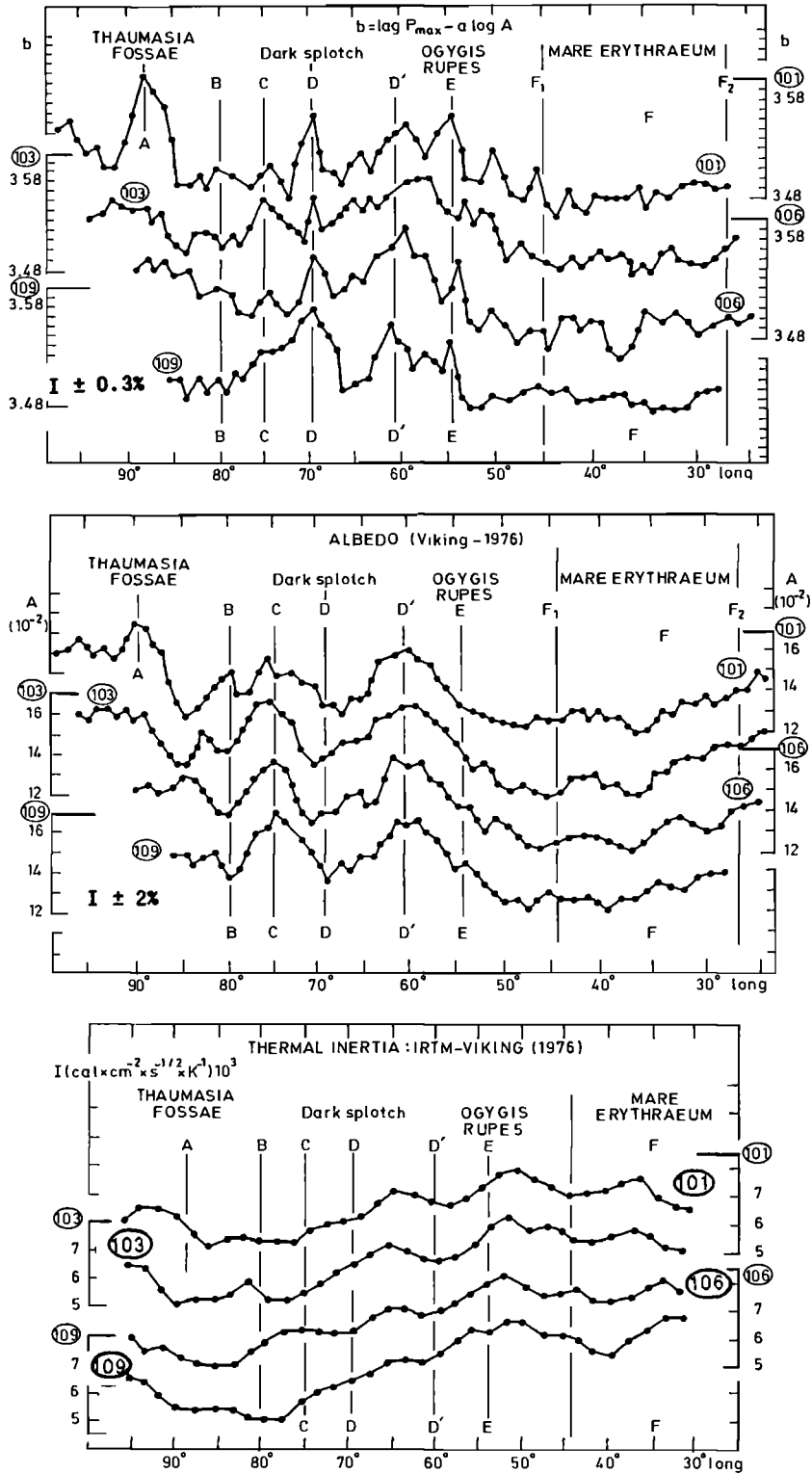


Fig. 1. Parameters  $b$ ,  $A$  and  $I$  plotted versus planetographic longitudes, for the four tracks 101, 103, 106, and 109 of Mars 5 VPM scans. (a) Polarimetric parameter  $b$  is the degree of polarization maximum corrected for albedo; it characterizes the grain size at the top surface of the martian soil. (b) Albedo parameter  $A$  is given for normal incidence and phase angle  $5^\circ$ ; it relates to the composition of the exposed top surface. (c) Thermal inertia parameter  $I$ , from Viking IRTM measurements; it characterizes the compaction, or the effective size of the particles in the subsurface, for the few decimeters below the top surface.

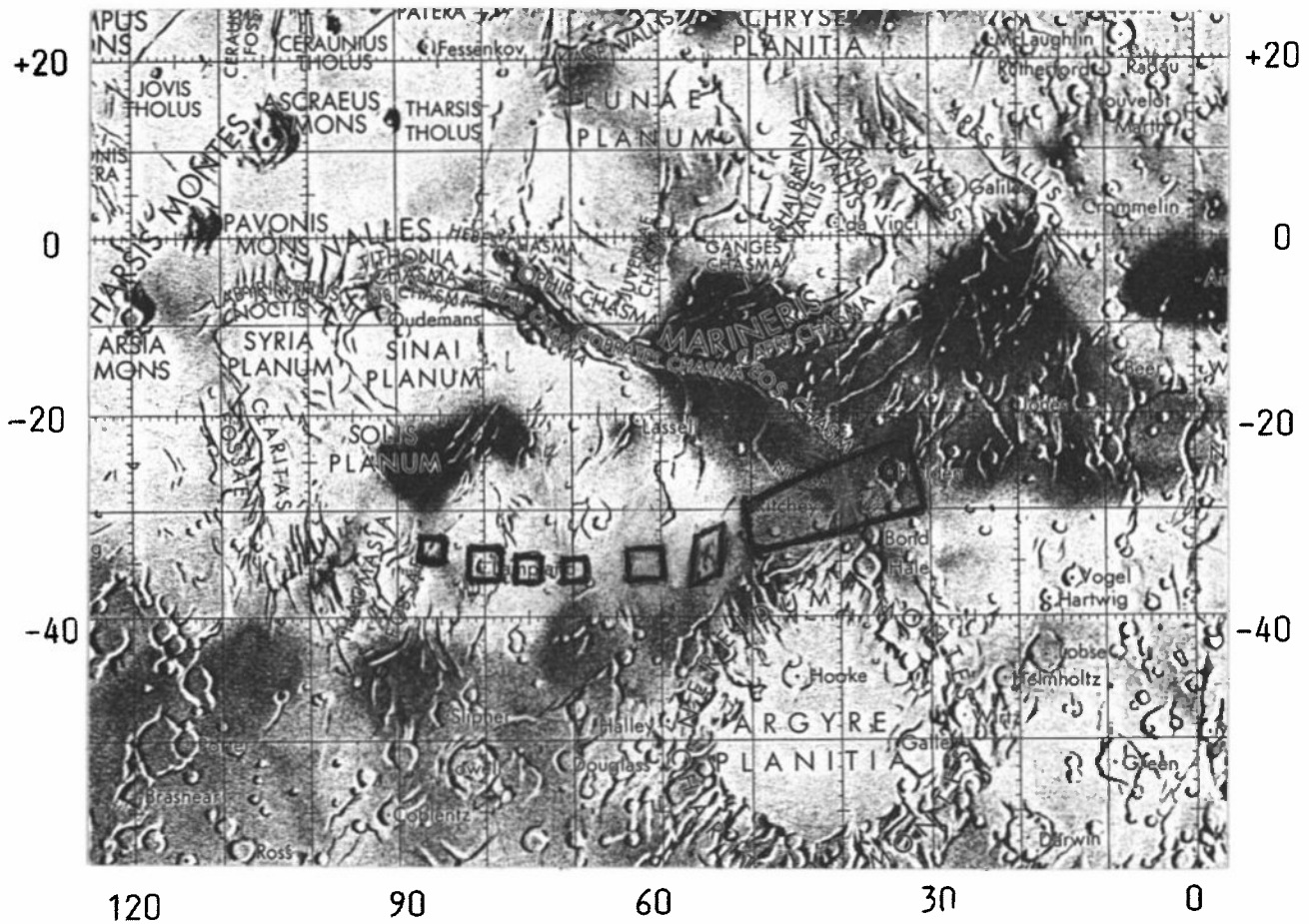


Fig. 2. The seven selected areas along the tracks racked by the Mars-5 scans. From left to right, the six first areas are all included in the bright-hued region Thaumasia. At right, the larger area extends entirely other the dark-hued region Mare Erythraeum.

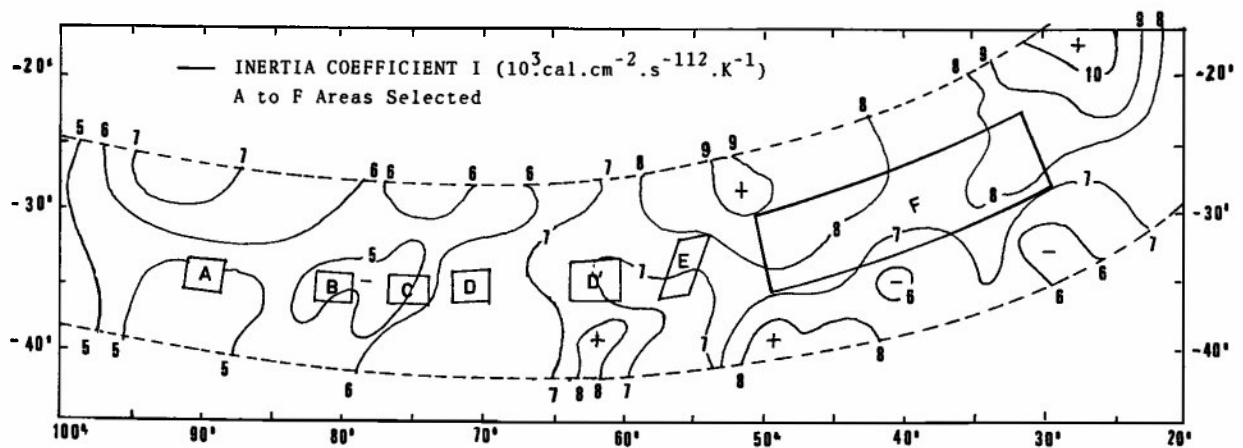


Fig. 3. Location and coordinates of the seven typical areas outlined over a map of the inertia coefficient *I* from Viking IRTM instrument (courtesy A. Peterfreund).

surfaces clean of dust. Then

$$P_{obs} = 1/A_{obs} [fX_{A_{grains}}X_{P_{grains}} + (1-f)A_{rocks}X_{P_{rocks}}]$$

The relationship between *I* and albedo *A* is shown given in Figure 8. Assuming the soil below

the top surface sensed by polarimetry is divided into pieces of approximately the same size, both Kieffer et al. [1977] and Vdovine et al. [1980] developed theoretical models in terms of an effective or average size of the soil components. The scale at right gives these sizes corresponding

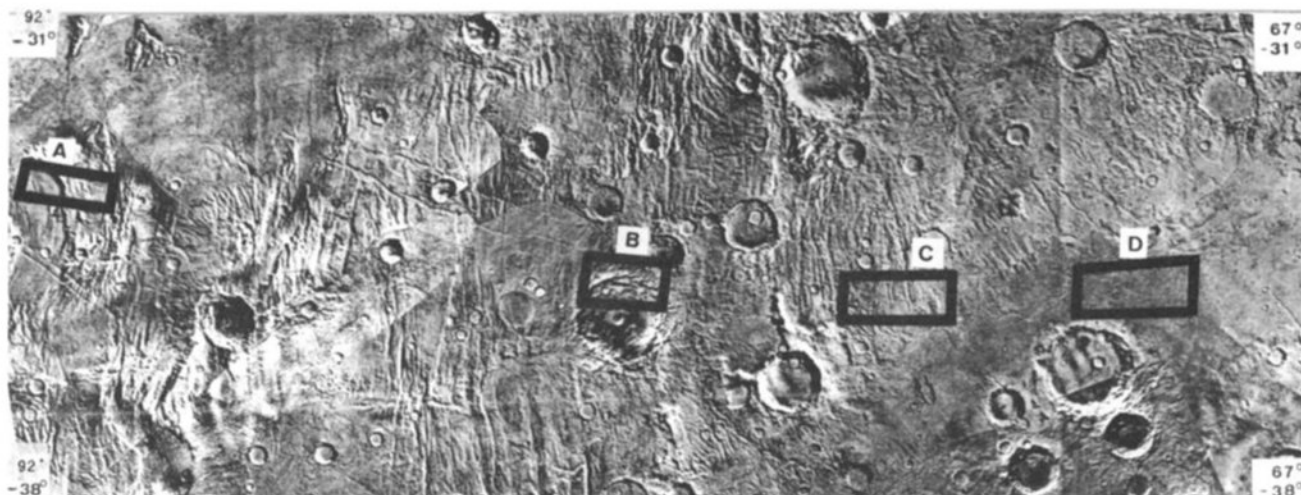


Fig. 4. Surface relief features in and around selected areas A to D from the NASA Viking Mars shaded relief maps.

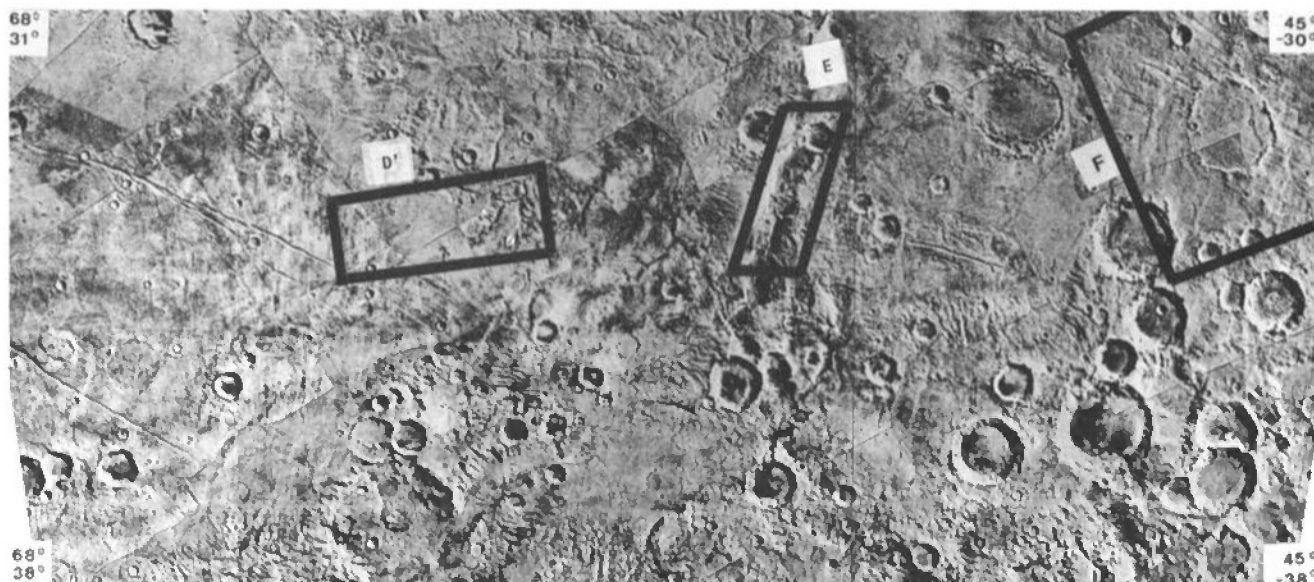


Fig. 5. Same as for Figure 4, for areas D', E, and F.

to the values of  $I$ , according to both theories. The agreement between both theories is well within a factor 2. The thermal insulation by the upper surface sensed by polarimetry is considered negligible, and the blocks of soil are assumed to be cohesionless. The relationship between thermal inertia and particle size has been discussed and refined by Jakosky [1986].

Figure 9 shows the relationship between the two parameters  $b$  and  $I$ , which is the size of the grains covering the top surface versus the size of the pieces in the underlying soil. Finally, the three parameters  $b$ ,  $I$  and  $A$  are related in a three-dimensional plot in Figure 10, in which each of the selected areas are represented by ellipsoids enveloping the measurements [see also Dollfus, 1991].

#### Soil Texture

##### Dark-Hued Region

In Figures 7 to 10, Mare Erythraeum (area F), is distinct from all the other areas and remains consistent over a broad region. Region F covers a wide area of  $240 \times 1200 \text{ km}^2$  (Figures, 2, 3, 5, and 6), and the measurements sampled the whole surface with a resolution of at least 60 km. The average albedo of 0.127 observed here is typical of dark surfaces on Mars [Focas, 1961] and corresponds to the southern part of the classical albedo feature Mare Erythraeum (Figure 2). Permanently observed at the telescope for more than a century, this region exhibits particularly few seasonal or long-term variations in its shape [de Mottoni,

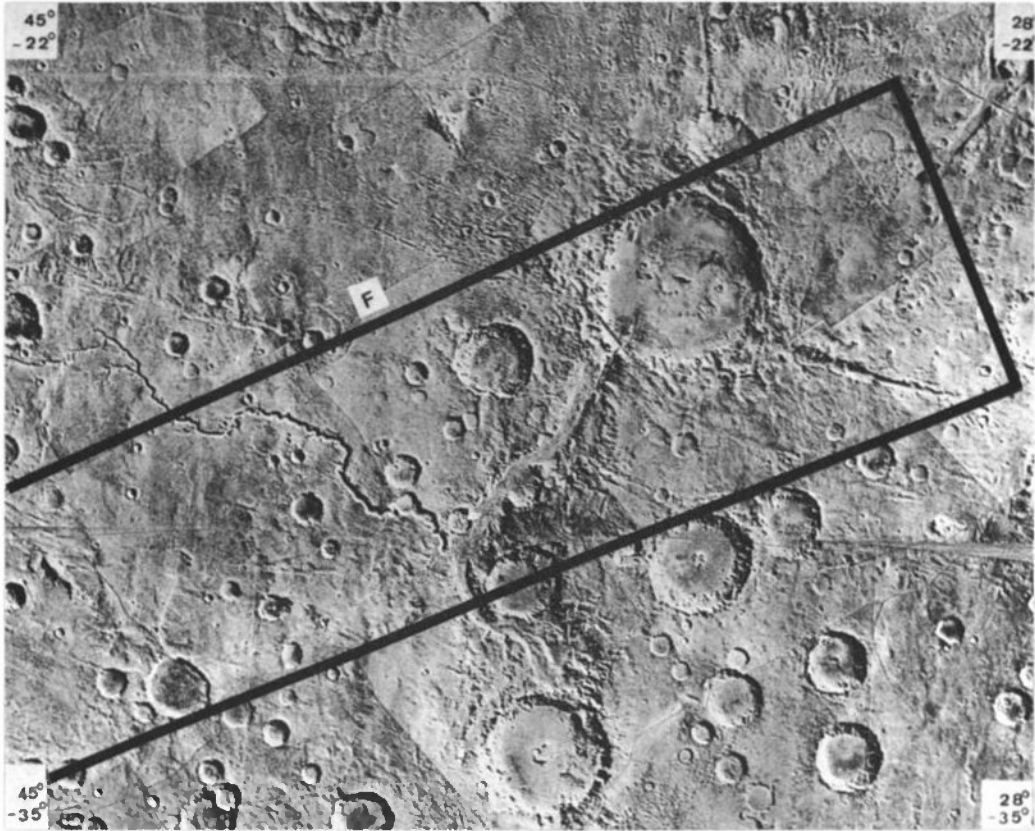


Fig. 6. Same as for Figures 4 and 5, for area F.

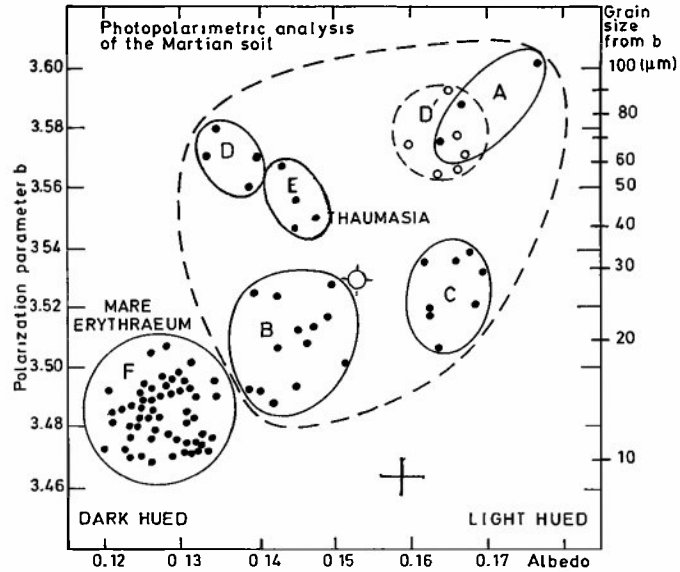


Fig. 7. Plot of the polarization parameter  $b$  versus albedo parameter  $A$ . Vertical scale at right: grain size corresponding to the  $b$  value of the scale at left, from laboratory calibration on sample made of non cohesive uniformly sized grains [Geake and Dollfus, 1986]. The dash-encircled domain includes all the measurements recorded over the Thaumasia region. The average values for Thaumasia are indicated by a crossed circle. Only those data corresponding to the selected areas are plotted here.

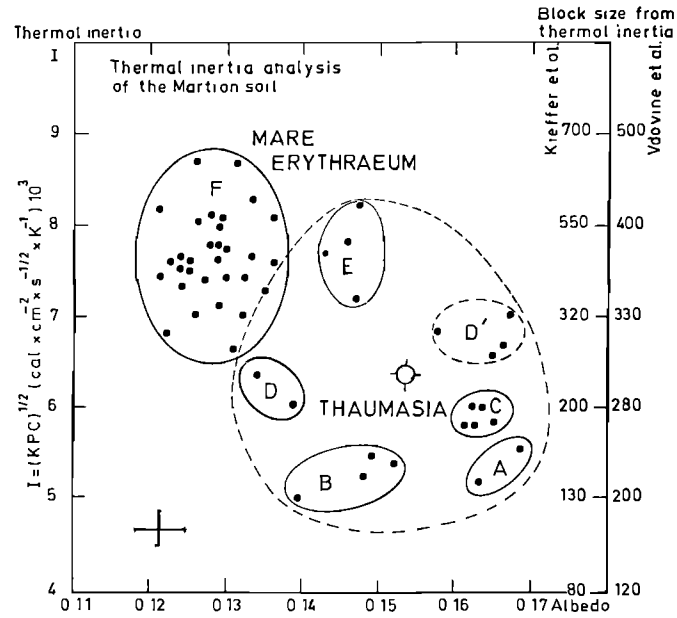


Fig. 8. Plot of the thermal inertia parameter  $I$  versus albedo  $A$ . Vertical scale at right: effective block size of surface soil components corresponding to the  $I$  values at left, according to models by Vdovine et al. [1980] and by Kieffer et al. [1977], assuming a soil divided in uniformly sized blocks piled up without cohesion. Dashed circled domain, same as for Figure 7.

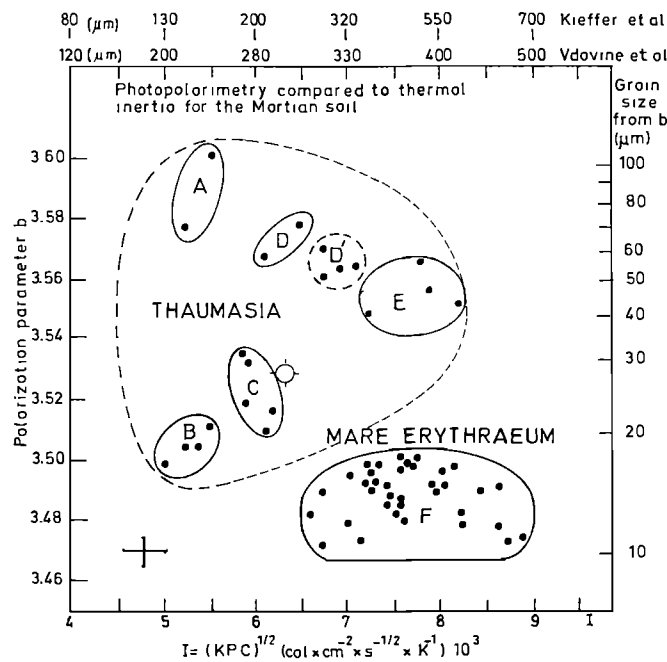


Fig. 9. Polarization parameter  $b$  versus thermal inertia  $I$ , same as for Figures 7 and 8.

1975; de Mottoni and Dollfus, 1982]. The area is representative of the most permanent dark features on the Martian surface.

The soil is characterized in the top its few decimeters below the surface by a thermal inertia

coefficient of 7.7, ranging from 6.5 to 9.0, which fits with the model of a particulate aggregates made of cohesionless pieces ranging in size from 250  $\mu\text{m}$  to 700  $\mu\text{m}$ . Recent corrections in the particle size scale analyzed by Haberle and







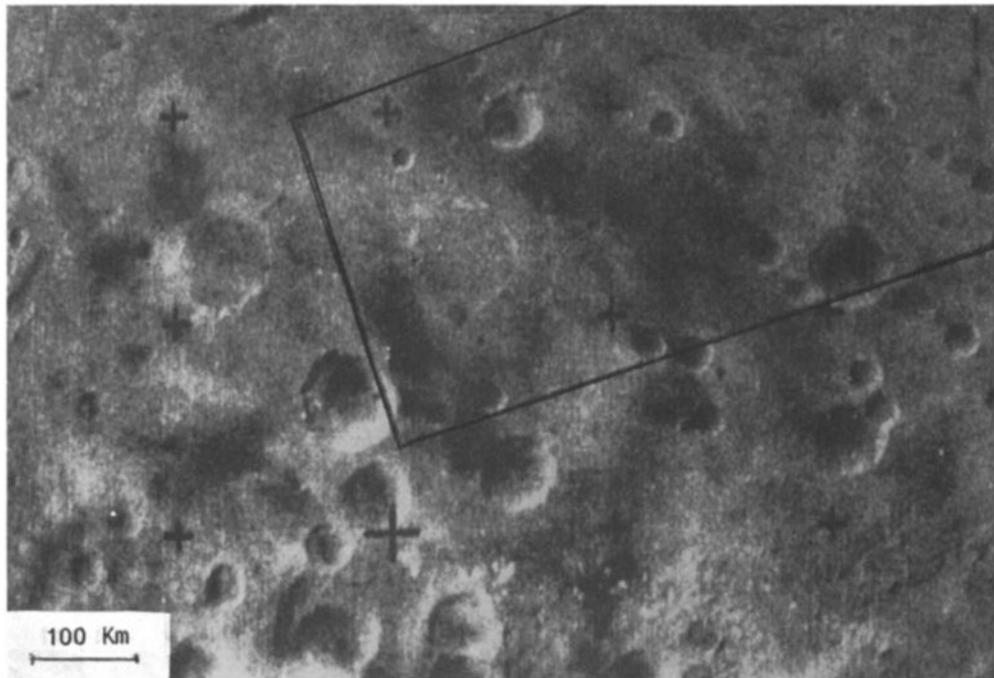


Fig. 11. Mars 5 large field camera images, February 17, 1974, orange filter, showing craters and albedo features over the western part of area F in Erythraeum (courtesy M.K. Naraeva and A.S. Selivanov).

Deschamps, 1986]. Near Uzboi Vallis, the rather high value of  $I = 10 \times 10^{-3}$  characterizes millimeter-size average particles, or  $f=18\%$  of the surface covered by competent materials; However, the top layer remains typical of the small size texture indicated by parameter  $b$ . Within the floor of Holden,  $I=8 \times 10^{-3}$  corresponds to effective grains of around  $400 \mu\text{m}$ , or  $f=12\%$  of the surface covered with competent materials, but again the mantling is present and none of the conductive material appears to be exposed dust-free at the surface. An area on the rim of crater Holden displays a very sharp increase of  $I$ , which could correspond to  $f=30\%$  of competent materials, but again the surface remains completely covered with the usual fine texture at visual wavelengths. Only the bottom of Nirgal Vallis displays a pronounced polarization anomaly, suggesting  $f=12\%$  of the surface with uncovered clean rocks [Dollfus and Deschamps, 1986].

Evidently all of Mare Erythraeum, apart for very localized exceptions, displays an overall texture with a near-surface soil dislocated in pieces much smaller than a millimeter in size. There are size variations from place to place, but the surface is nowhere finely comminuted to depths of even centimeters. However, these fragments are everywhere covered, coated or mantled by a finer medium, spread very uniformly, comprised of small dark grains of 0.127 average albedo and  $14 \mu\text{m}$  mean size, with local variations only from  $10 \mu\text{m}$  to  $20 \mu\text{m}$ , all over an area of  $3 \times 10^5 \text{ km}^2$ .

#### Light-Hued Region

All the other measurements within the study area correspond to the bright-hued terrain

Thaumasia (Figure 2). Although the strip scanned in Thaumasia is longer and narrower, the whole region sampled has approximately the same surface area as the dark Mare Erythraeum, and the total number of measurements is also about 100.

In contrast to Erythraeum, the soil properties in Thaumasia are far more diversified. In the parameter plots of the Figures 7, 8, and 9, all of the measurements from Thaumasia are encircled by a dashed line (but only those points from the selected areas A to E are shown in these diagrams). These domains are far more extended in parameter space than for the dark Mare Erythraeum, indicating a greater diversification in the soil properties. They are displaced from and do not overlap with their Erythraeum counterparts, attesting to different soil textures in both regions for the subsurface as well as the exposed top layers.

Statistics produce a mean thermal inertia coefficient of  $I = 6.3 \pm 1.0$  ( $1\sigma$ ) with extreme values of 4.9 and 8.5, as compared to 7.8 for Mare Erythraeum. These results indicate soil fragments on the average twice smaller in size than those in Mare Erythraeum, around  $300 \mu\text{m}$  in the calibration scales given here, but with local variations of from  $100 \mu\text{m}$  to  $600 \mu\text{m}$ . The top surface layer, orange in color and of average albedo 0.153, is characterized by  $b=3.529 \pm 0.029$  ( $1\sigma$ ), which implies grains of average size  $30 \mu\text{m}$ . These bright grains are more than twice the size of the  $14 \mu\text{m}$  grains of albedo 0.125 in Mare Erythraeum, with large local variations in size, ranging from  $15 \mu\text{m}$  to  $100 \mu\text{m}$ . The dichotomy in behavior between the dark Erythraeum and the light Thaumasia soils is evidenced in the three-dimensional plot of Figure 10.

### Selected Area in Thaumasia

Area C is taken first, because it is representative of the average soil texture over Thaumasia, although with slightly lighter albedo (0.163). The terrain extends east of the partly buried rim of an old crater (Figure 12). There are degraded grabens and scarps, but the area appears essentially smooth and may be mantled.

The value  $b = 3.520$  (Figure 7) indicates that the top exposed surface is made up of grains from 20 to 40  $\mu\text{m}$  in diameter. When the area was scanned for polarimetry with a footprint size  $20 \times 40 \text{ km}^2$ , small scintillation effects in the signal suggested possible Fresnel reflections from rock clusters with clean surfaces [Dollfus et al., 1983]. If such is the case, a model can be fitted with grains 15  $\mu\text{m}$  in size and 3.3% of the total surface with exposed bare rock surfaces deprived of dust. The abundance of rocks exposed on the ground in this area is estimated by Christensen [1986b], on the basis of temperature contrasts in the IRTM measurements, to cover of about 5% of the total surface. The real case is probably between these two results.

The subsurface is characterized by  $I = 6.0$ , which implies effective particulates from 150 to 300  $\mu\text{m}$  in diameter (according to the particle scale adopted), possibly smaller if atmospheric correction and cementing are considered, possibly larger if the surficial layer of small grains is

thick enough to contribute significantly to the thermal insulation.

Area B (Figure 4) refers to the north rim of the large crater Lampland [Dollfus et al., 1983, see Figures 17-19]. Despite a totally different geomorphological appearance, area B discloses some resemblance in soil properties with area C. The top surface layer, although somewhat darker ( $A = 0.145$ ), appears to be also made of grains from 15 to 30  $\mu\text{m}$  in diameter. Polarimetric scintillation again suggests some possible effects attributable to dust-clean rocks [Dollfus et al., 1983], but with a maximum of 3.5% rocks at the surface if the dust grains are as small as 15  $\mu\text{m}$ . The inertia coefficient  $I = 5.3$  characterizes underground fragments 150 to 250  $\mu\text{m}$  in size, comparable in size to that of terrain C, despite the drastic geological and geomorphological differences between these two locations.

Area D (Figure 13) is located on a dark splotch near crater Babakin (longitude  $72^\circ$ , latitude  $-36'$ ). Such dark features are attributed to deflation by saltation and dust removal by eolian effects [Bagnold, 1941]. It could result from the local removal of a mantling of light dust, exposing an underlying dark terrain related to mare materials. The average albedo of the splotch is 0.137, slightly brighter than region F in Mare Erythraeum ( $A = 0.127$ ), although there are some darker and brighter patches within area D [see Dollfus et al., 1983, Figure 7].

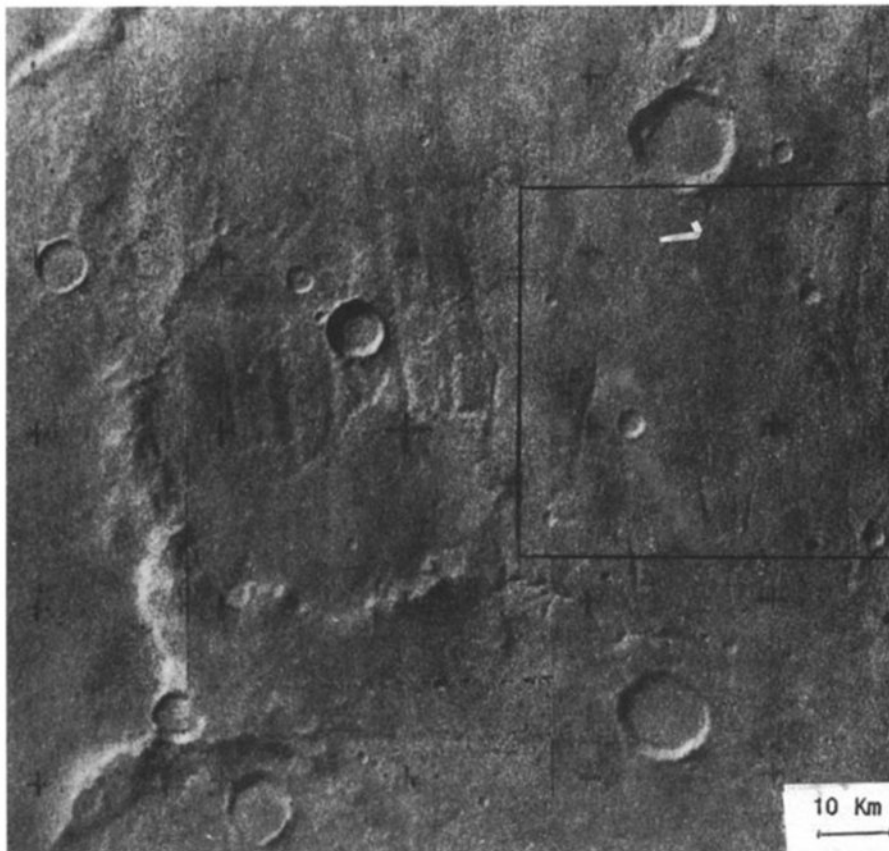


Fig. 12. Mars 5 high-resolution camera image of area C in Thaumasia, February 26, 1974, orange filter (courtesy N. Naraeva and A.S. Selivanov).

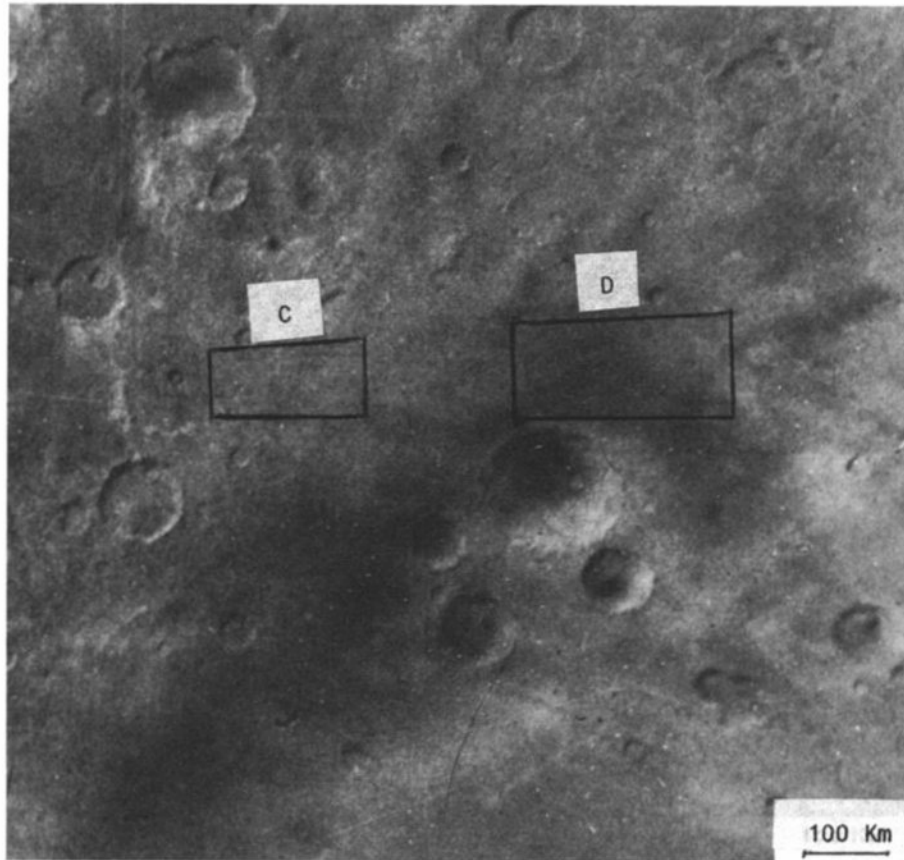


Fig. 13. Mars 5 field camera image, February 26, 1974, red filter, showing areas C and D, framed over a dark splotch, north of crater Babakin (courtesy M.K. Naraeva and A.S. Selivanov).

The subsurface soil, with  $I=6.2$ , fits an interpretation with particles 200 to 300  $\mu\text{m}$  in size (subject to the corrections stated above). There is not a clear increase of  $I$  in this aeolian feature relative to its surroundings, as noted by *Zimelman and Leshin [1987]* for similar features in the Elysium area. The exposed top surface, with  $b=3.570$ , is characterized by coarse grains, 50 to 80  $\mu\text{m}$  in size, definitely larger than for regions B and C (a model assuming that 15  $\mu\text{m}$  mare-type grains need 10% exposed clean rocks at the surface to produce the polarization observed and seems unrealistic). Alternatively, a thick layer made of 80  $\mu\text{m}$  grains, with proper cementing to account for parameter  $I$ , may account for all of the parameters. In this specific dark patch, the exposed surface is made of larger grains than elsewhere. Despite an albedo similarly, the soil does not have the texture of the permanent dark region (F) in Mare Erythraeum, which is made of coarser underground granular regolith and a more finely divided top surface.

Area A is framed on the highly tectonized Thaumasia Fossae and has a relatively bright albedo 0.170. This terrain is densely covered with rocks, 15% of its surface, according to *Christensen [1986 b]*. The grain size surface parameter  $b=3.590$  is the highest of all the areas measured. For a homogeneous superficial powder, grain sizes from 70  $\mu\text{m}$  to more than 100  $\mu\text{m}$  are

implied. If the grains are 15  $\mu\text{m}$ , then 12% of the surface has to be occupied by exposed rocks clean of dust.

The subsurface below this coarse powdered layer has a thermal inertia coefficient  $I=5.4$ , which should be somewhat decreased to correct the effect of the rocks [*Christensen, 1986 b*], and characterizes a granular regolith slightly finer than average. It is essentially the top surface which is most modified in this very rugged area.

Area E (Figure 5) is a scarp, Ogygis Rupes. There is a sharp increase of polarization at the bottom of the fault indicating larger grains (40 to 70  $\mu\text{m}$  in our present estimate) or isolated exposure of unmantled rocks [*Dollfus et al., 1983*]. There is also a concentration of rocks, according to *Christensen [1986 a,b]*. Four values of the inertia coefficient, with a resolution of 60 km, which is twice the width of the fault, range from 7.2 to 8.4; the true value for the scarp bottom itself is probably far larger, in compliance with an accumulation of boulders and rocks.

#### Interpretations

A simple crude model for the soil texture derived from these multiple observations is with two-size composite grains (Table 1). Such grains are sketched in the Figure 14, approximatively at

TABLE 1. Mars : Surface texture and Granulometry

Region	Code	A % ±2%	b ±0.3%	I ±0.5%	Rock Abundance [Christensen, 1986a, b]	Soil Texture From Thermal Inertia	Exposed Surface From Polarimetry
Mare Erythraeum Large dark albedo feature	F	12.7	3.485	7.7	uneven few percent to 10% of the surface covered with rocks	divided in regolith with pieces 300-600 μm, smaller if somewhat cemented	ubiquitous covering with very small grains 15 μm in size
Thaumasia fossae	A	17.0	3.590	5.4	15%	regolith with pieces around 150-250 μm, smaller if cohesive, larger if top layer not thin	light-hued grains, 70-100 μm in size and smaller; maximum of few percent surface could be bare rocks
Rim of crater Lampland	B	14.5	3.510	5.3	few percent	same as for A	medium dark small grains of maximum size 30 μm
Old fractured terrain, mantled	C	16.3	3.520	6.0	few percent	same as A and B, slightly coarser pieces 180-300 μm	light grains 20-40 μm and smaller; Fe or not exposed clear rock surfaces
Dark splotch near crater Babakin	D	13.7	3.570	6.2	not resolved	same as C, with pieces 200-300 μm or grains 80 μm same as surface, partly cemented.	dark coarse grains 50-80 μm could be the same as for soil underneath, or some exposed bare rocks
Ogygis rupes	E	14.5	3.560	7.2 to 8.4	15%	field of large pieces, rocks or blocks	grains around 50 μm or less

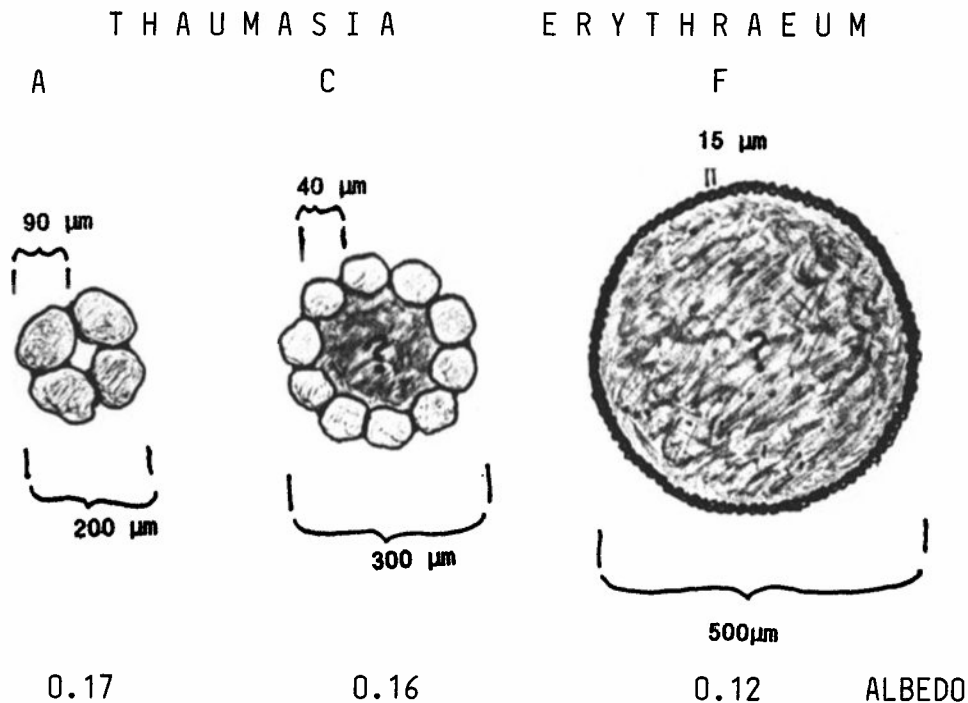


Fig. 14. Two-size composite grains model. Each grain is assumed to be made of a core, enveloped by smaller grains. Polarimetry and albedo characterize the small surface grains. Thermal inertia refers to the size of the whole composite grain. In the dark-hued region Erythraeum (at right), large grains, half a millimeter in size, are wrapped by cohesive small  $15\ \mu\text{m}$  size dark particles. For light-hued Thaumasia, the typical area C (at center) is made of grains of a third of millimeter in diameter, enveloped by bright orange  $40\ \mu\text{m}$  grains. The dimensions of these orange grains are variable for place to place over the Thaumasia region. For area A (at left) these orange grains are more than twice as large as in area c and assembled in smaller composite grains. All the sizes are shown approximately at the same scale. The soil, in this simple model, is assumed to be made of cohesionless piles of relevant grains.

the same scale, for Erythraeum and for two cases in Thaumasia. These grains are piled up to produce the soil observed by both the VPM and IRTM experiments.

In Erythraeum, the composite grains would be about  $500\ \mu\text{m}$  in diameter, coated with  $15\ \mu\text{m}$  dust particles. The dust has an albedo 0.13, its composition documented by the reflectance spectra from the dark-hued areas [Singer *et al.*, 1979, 1990; Singer, 1980, 1985; Bell *et al.*, 1989]. The core may be a solid piece, or an aggregation of cemented smaller grains, but its composition can not be sensed due to the adhering dust grains. The grain interior could be made of the same material as the dust, in which case the pieces are wrapped in their own debris, or it could be of a different nature. The Erythraeum near-surface soil could be made of a pile of such composite grains with a certain dispersion in size, with the small dark particles stuck cohesively at their surfaces (Figure 15a, left).

In Thaumasia, the grains are of a different nature from those in Erythraeum and they are not of the same size in every place. For the typical area C, the assemblage could consist of  $40\ \mu\text{m}$  grains of albedo 0.16 enveloping an unknown core to produce granules  $300\ \mu\text{m}$  in diameter (Figure 14,

center). For area A, larger  $90\ \mu\text{m}$  grains could be cemented to produce conglomerate grains  $200\ \mu\text{m}$  in size (Figure 14, left). In the piling up such grains, there is apparently a surface layer of the small grains (Figure 15a, right).

The texture could include small grains attached to the larger pieces, plus small grains intermixed, and a top layer of free small grains, with a distribution of grain sizes. The small bright surface grains could make the "drift material" identified by Mutch *et al.* [1976 a,b] and by Moore and Jakosky [1989] at the Viking landing sites, the larger pieces being more like the "crusty to cloddy" material.

A thicker upper layer of grains requires larger pieces underneath, to maintain the observed thermal inertia (model I, Figure 15b). The upper layer may include clean exposed rock surfaces, but the surface grains would then have to be smaller to compensate for the high polarization produced by the bare rocks (model II).

#### Speculations

##### Nature of the Dark Terrains

The striking uniformity of the small dark particles all over the Erythraeum low-albedo

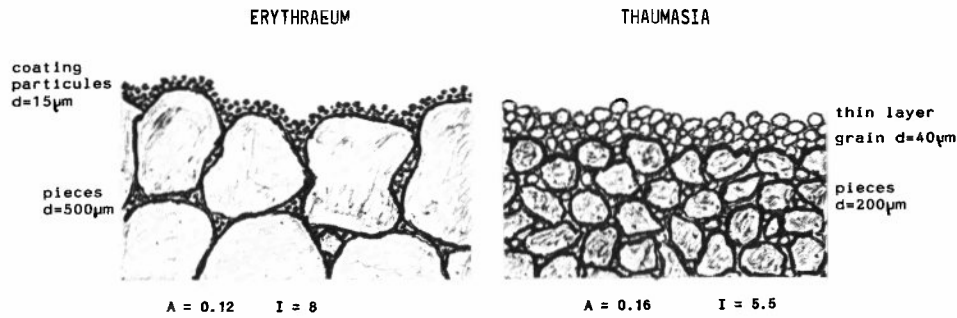


Fig. 15a. Surface layer models. Polarization is assumed to refer to an upper layer of small grains covering everywhere a regolithic soil made of piles of larger fragments. For Erythraeum, the construct is not very different from the model of the Figure 14. For Thaumasia, the orange bright grains are assumed to be intermixed with the large pieces and to cover the whole surface with a noncohesive layer. If the surface layer has a thickness of a centimeter or more, its thermal insulation requires a compensation of the thermal response by a granular regolith made of larger pieces.

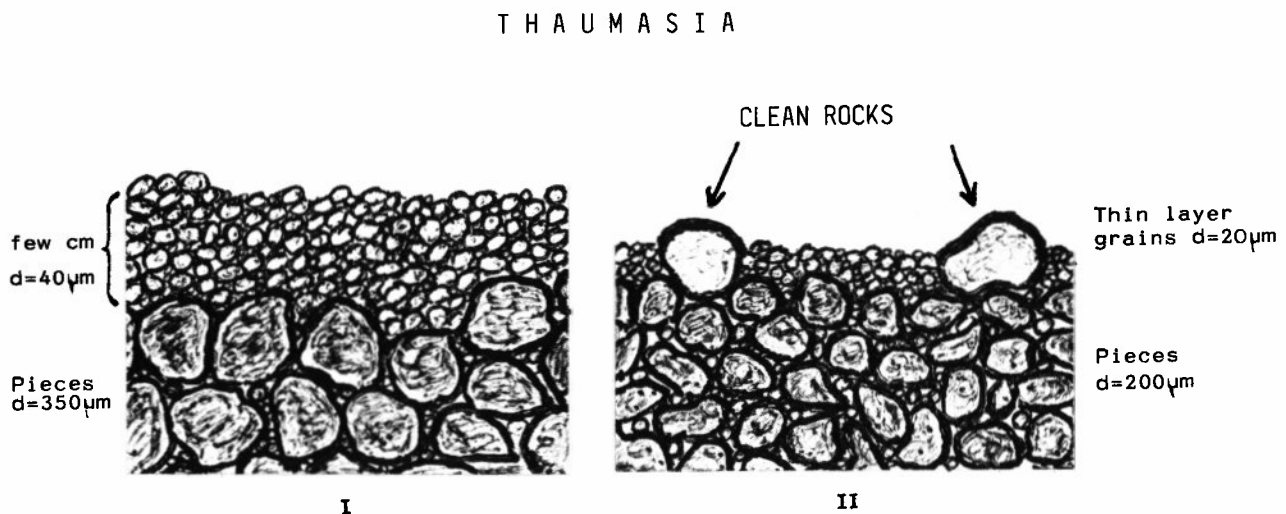


Fig. 15b. Same as Figure 15a, for models I and II. If there are exposed rocks or large compact pieces, with some parts of their surfaces deprived of small grains, the increased polarization requires a compensation by smaller grains in the surface layer (model II).

region may suggest a late dark dust deposition event which would cover a large region with an uniform dust deposit, giving a consistent polarimetric signal. However, such dark dust deposits would not be consistent with the numerous observations of bright dust being raised from the surface by localized dust storms. Reflectance spectra shows low-albedo regions as having stronger absorption features, representative of mafic materials [Singer, 1980]. On the basis of terrestrial analogs to the Martian soil spectral and magnetic properties, Morris and Lauer [1990] and Morris et al. [1990] proposed the dark materials to be made of dark merocrystalline tachylite basalt, plus small opaque grains of

titanomagnetite. We speculate that the large pieces responsible for the  $I$  parameter are the tachylite basalt material and that the material which is cohesively coating these large pieces are the small grains of Fe-Ti oxides, almost black. The polarimetric signal (parameter  $b$ ) is then produced by the small titanomagnetite grains wrapping the larger pieces, as is the overall albedo (parameter  $A$ ).

#### Nature of the Bright Terrains

In the bright area Thaumasia, the surface grains are shown by photopolarimetry to be in the size range of 20 to 60 µm, although there is

likely a distribution sizes of the polarimetric signal characterizing essentially the largest grains. These particles are orange in color. They are overlaying and possibly mixed with a subsurface granular regolithic soil made of pieces a small fraction of millimeter in size (fine sand). The small orange surface grains are probably the brown basalt glass particles (sideromelane), which were identified by *Morris et al.* [1990] on highly weathered (palagonitized) volcanic samples from Hawaii that simulate the spectral and magnetic properties of the Martian soil.

#### *Dust Storm Source Terrains*

The dust storm initial phases, before growing to a global scale, are known to occur preferentially, over specific, well-identified areas which are of bright or intermediate albedo. These major dust storm source regions are Hellas-Iapigia, Isidis, Phaethontis and Argyre-Thaumasia [*Gierash*, 1974; *Zurek*, 1982; *Martin*, 1984; *Dollfus et al.*, 1984a,b; *Ebisawa and Dollfus*, 1986]. Thaumasia is typically representative of such a dust storm initiation area.

In fact, despite an overall Martian atmosphere particularly free of suspended dust during the period of the VPM polarimetric records [*Dollfus et al.*, 1977], and the dust storm season being definitely over, several dust-raising events have been observed in our polarimetric scans over Thaumasia [*Santer et al.*, 1985]. The selected area D' is a typical case, where the dust haze was visible in the images simultaneously taken with the Mars 5 cameras [see *Dollfus et al.*, 1985, Figure 9b].

Soil surfaces of the Thaumasia type appear to be required to permit the injection of dust grains into the atmosphere, in addition to relevant seasonal, meteorological, thermal, and topographic environments: regolith made of small sand-sized pieces and a population of smaller dust-sized grains which are intermixed and cover the surface. Such a texture appears to be the right one to generate the saltation process required to eject the smaller grains into the air during a strong wind: aerodynamical drag displaces the sand particles at the surface. Subsequent impacts of the saltating sand kick the smallest particles into the air, which are then able to stay suspended in the atmosphere and be transported by the wind [*Greeley et al.*, 1976, 1980, 1981]. Large deposition surfaces such as Arabia or Amazonis are too fine-grained and probably too smooth to initiate the saltation process required to kick the small grains up into the air [*Zimelman and Kieffer*, 1979; *Christensen*, 1982, 1986a]. Dark areas, assumed in our model to be made of coarse grains wrapped with titanomagnetite particles, have sizes too large and small particles too cohesive to be lifted up into the air.

#### *Particle Reservoirs for Dust Storms*

There is a problem of perennality for areas like Thaumasia to repeatedly supply dust for dust storms. Although the local dust-raising events redeposit some particles nearby, the global storms spread the dust all over the planet, and the

result is a net loss from the supplying area. The deflation should stop when the reservoir supplying the small grains is exhausted in the soil, or when a layer of different aerodynamic texture emerges at the surface.

Of special interest along this line is the dark splotch of area D. Here, as a result of local elimination of the upper layer of orange grains, a darker layer is reached. The thermal inertia is locally as large as for Erythraeum and corresponds to model grains of several hundred micrometers in size, able to support the saltation process at the surface, which removed most of the overlying bright grains. However, in contrast with the very fine dark particles detected by polarization in Erythraeum, and attributed to the wrapping of the large pieces by black titanomagnetite particles, the polarimetric signal in area D characterizes larger dark grains, or possibly a texture similar to Erythraeum but with several percent of the surface occupied by exposed clean bare rock elements. Such material could locally resupply fine dust as it weathers from the darker, less weathered material just exposed.

#### *Permanence of the Dark Terrains*

The large dark configurations which are observed at the surface of Mars appear at the telescope as permanent features, at least over the last two centuries. Only some small and often recurrent variations in shape or contrast are noted, which have been surveyed and analyzed in detail [*de Mottoni*, 1975; *de Mottoni and Dollfus*, 1962]. However, these dark terrains are exposed to the deposition of the bright dust particles raised into the atmosphere by dust storms. Progressively, these dark surfaces could be covered by a mantling of bright small grains. A mechanism is required to clean these areas from dust accumulation.

The texture of the dark terrains which emerges from the present work goes along with a process of saltation advocated to remove the dust, from dark regions [*Christensen*, 1982, 1986a, 1988]. During periods of strong wind, the large grains which compose the soil have the proper dimension to initiate saltation, which permits the small dust particles added at the surface by global storms to be ejected once again and transported elsewhere by the wind, thus cleaning the region. The small black titanomagnetic grains which are part of the composition of the soil are responsible for the low albedo of the region, but they are strongly adhered to the surface of the larger pieces, so that the saltation process cannot lift them into the air and they stay in place, attached to the large pieces.

#### *Nature of the Dust Storm Particles*

There are convincing arguments to consider the bright regions of Mars as areas of deposition for the dust raised into the air at the occasion of global storms [*Kieffer et al.*, 1977; *Zimelman and Kieffer*, 1979; *Christensen*, 1982, 1986a]. Once dust begins to accumulate, the existing material which may be subjected to the saltation process may become buried, and the rate of dust removal is further reduced. Major areas of deposition are the bright regions Arabia and Elysium and the area called Tharsis (which is, in fact, Amazonis). The model implies that the dust which is raised and



transported during storms is exclusively made of the bright orange grains; the dark material which makes the permanent or recurrent dark features at the surface of Mars is supposed to be never lifted in the air. At least, such dark dust in suspension has not been observed on Mars.

On Earth, dark tachylite grains are formed during volcanic ash eruptions ("nuées ardentes"). Bright sideromelane grains are also produced in pyroclastic eruptions, depending of the evolutionary state of the source magma. The sideromelane-rich particles are known to be more sensitive to weathering than the tachylite grains; hydrated ferric oxides are formed, red in color, essentially hematite in composition, which convert the grains into palagonite [Morris et al., 1990]. For the case of Mars, other weathering processes are also under consideration [Huguenin, 1974]. There is a possibility that under current Martian conditions, bright orange weathered material is the only one able to be comminuted into non cohesive small grains and thus able to be placed in suspension in the air.

The dark tachylite material could produce a natural physical texture in larger grains only, hundredths of micrometers in size, with associated small titanomagnetite dust particles adhering so firmly to these grains that they are unable to be removed by saltation. If these two circumstances are achieved on Mars under the natural processes at work in the magmatic, chemical, and physical conditions present in the Martian environment, then the dust raised from the ground during dust storms should be made of bright grains only, as observed, with a composition of orange weathered palagonite.

**Acknowledgments.** The authors are grateful to the Soviet Academy of Sciences and its Space Science Institute IKI and to the French Centre National d'Etudes Spatiales for the operation of the photopolarimeter VPM on board spacecraft Mars 5, in close collaboration with L.V. Ksanfomaliti all along this Soviet-French project. M.K. Naraeva and A.S. Selivanov produced the images of the Martian surface recorded simultaneously by the Mars 5 cameras. A. Peterfreund supplied some of the early IRTM data, processing them and stimulating important discussions. Polarization analysis and interpretation problems were deciphered along a long-term cooperation with J.E. Geake, L.M. Dougherty, M. Wolff, and S. Ebisawa. Atmospheric analyses were conducted with R. Santer. We had many laboratory discussions with E. Grin, D. Crussaire, and N. Cabrol, with comments by J.F. Bell and R.V. Morris and inspirations from P.R. Christensen, R.R. Greeley, R.M. Haberle, and B.H. Jakosky. Proportions of this work were carried out while J.R.Z. was a Visiting Scientist at the Lunar and Planetary Institute, which is operated by the Universities Space Research Association under grant NASW-4574 with the National Aeronautics and Space Administration. The authors are grateful for constructive comments by Paul Helfenstein and by another anonymous colleague, acting as referees.

#### References

- Bagnold, R.A., *The Physics of Blown Sand and Desert Dunes*, pp. 265, Methuen, London, 1941.
- Bell, J.F., III, McCort, T.B. and Lucey, P.G., Imaging spectroscopy of Mars (0.4-1.1  $\mu\text{m}$ ) during the 1988 opposition, *Proc. Lunar Planet. Sci. Conf.*, 20th, 479-486, 1989.
- Christensen, P.R., Martian dust mantling and surface composition: Interpretation of thermophysical properties, *J. Geophys. Res.*, 87, 9985-9998, 1982.
- Christensen, P.R., Regional dust deposits on Mars: Physical properties, age and history, *J. Geophys. Res.*, 91, 3533-3545, 1986a.
- Christensen, P.R., The spatial distribution of rocks on Mars, *Icarus*, 68, 217-238, 1986b.
- Christensen, P.R., Global albedo variation on Mars: Implication for active aeolian transport, deposition and erosion, *J. Geophys. Res.*, 93, 7611-7624, 1988.
- de Mottoni, G., The appearance of Mars from 1907 to 1981: Graphic synthesis of photographs from the IAU Center at Meudon, *Icarus*, 25, 296-332, 1975.
- de Mottoni, G. and A. Dollfus, Surface marking variations of selected areas on Mars, *Astron. Astrophys.*, 116, 323-331, 1982.
- Deschamps, M. and A. Dollfus, Granulométrie du sol de Mars par photopolarimétrie, *Bull. Soc. Géol. Fr.*, 8, 59-64, 1987.
- Dollfus, A., The nature of the surface of Mars, *Publ. Astron. Soc. Pac.*, 70, 56, 1958.
- Dollfus, A., Sensing the physical properties at the Martian surface in *The Environmental Model of Mars*, Cospar Colloquia, vol. 2, edited by K. Szego, pp. 101-104, Pergamon, New York, 1991.
- Dollfus, A. and M. Deschamps, Grain-size determination at the surface of Mars, *Icarus*, 67, 37-50, 1986.
- Dollfus, A. and J. Focas, La planète Mars: la nature de sa surface et les propriétés de son atmosphère, d'après la polarisation de sa lumière, I, Observations, *Ann. Astrophys.*, 2, 63-74, 1969.
- Dollfus, A., J. Focas and E. Bowell, La planète Mars: La nature de sa surface et les propriétés de son atmosphère, d'après la polarisation de sa lumière, II, La nature du sol, *Ann. Astrophys.*, 2, 105-121, 1969.
- Dollfus, A., L.V. Ksanfomaliti and V.I. Moroz, Simultaneous polarimetry of Mars from Mars-5 spacecraft and ground-based telescopes, *Space Res.*, XVII, 667-671, 1977.
- Dollfus, A., M. Deschamps and L.V. Ksanfomaliti, The surface texture of the Martian soil from the Soviet spacecrafts Mars-5 photopolarimeters, *Astron. Astrophys.*, 123, 225-237, 1983.
- Dollfus, A., S. Ebisawa and E. Bowell, Polarimetric analysis of the Martian dust storms and clouds in 1971, *Astron. Astrophys.*, 131, 123-136, 1984a.
- Dollfus, A., E. Bowell and S. Ebisawa, The Martian dust storm of 1973: A polarimetric analysis, *Astron. Astrophys.*, 134, 343-353, 1984b.
- Ebisawa, S. and A. Dollfus, Martian dust storms at the early stage of their evolution, *Icarus*, 75, 75-82, 1986.
- Focas, J.H., Etude photométrique et polarimétrique des phénomènes saisonniers de la planète Mars, *Ann. Astrophys.*, 24, 309-325, 1961.
- Geake, J.E. and A. Dollfus, Planetary surface texture and albedo from parameter plots of optical polarization data, *Mon. Not. R. Astron. Soc.*, 218, 75-91, 1986.
- Gierash, P.J., Martian dust storms, *Rev. Geophys.*, 12, 730-734, 1974.
- Greeley, R.R., B.R. White, R.N. Leach, J.D. Iversen and J.B. Pollack, Mars: Wind friction speeds for particles movements, *Geophys. Res. Lett.*, 3, 417-420, 1976.
- Greeley, R.R., R.N. Leach, B.R. White, J.D. Iversen and J.B. Pollack, Threshold wind speeds for sands on Mars: Wind tunnel simulations, *Geophys. Res. Lett.*, 7, 121-124, 1980.
- Greeley, R.R., B.R. White, J.B. Pollack, J.D. Iversen and R.N. Leach, Dust storms on Mars: Considerations and simulations, *Spec. Pap. Geol. Soc. Am.*, 186, 101-121, 1981.
- Haberle, R.M. and B. Jakosky, Atmospheric effects on the remote determination of thermal inertia on Mars, *Icarus*, 90, 187-204, 1991.
- Huguenin, R.L., The formation of goethite and hydrated clay minerals on Mars, *J. Geophys. Res.*, 79, 3895-3905, 1974.
- Jakosky, B.M., On the thermal properties of Martian fines, *Icarus*, 66, 117-124, 1986.

- Jakosky, B.M. and P.R. Christensen, global duricrust on Mars: Analysis of remote-sensing data, *J. Geophys. Res.*, *91*, 3547-3559, 1986a.
- Jakosky, B.M. and P.R. Christensen, Are the Viking lander sites representative of the surface of Mars?, *Icarus*, *66*, 125-133, 1986b.
- Kieffer, H.H., T.Z. Martin, A.R. Peterfreund, B.M. Jakosky, E.D. Miner and F.D. Palluconi, Thermal and albedo mapping of Mars during the Viking primary mission, *J. Geophys. Res.*, *82*, 4249-4291, 1977.
- Ksanfomaliti, L.V., V.I. Moroz and A. Dollfus, (in russian) *Kosm. Issled.* *13*(1), 92-98, 1975. (English transl. UDC, Polarimetric Experiment with Mars 5, 543.47:523.43.)
- Ksanfomaliti, L.V. and A. Dollfus, Polarimetry and photometry of Mars from Mars-5 probe, *Space Res.*, *XVI*, 975-981, 1976.
- Martin, T.Z., Mean thermal and albedo behaviour of the Mars surface and atmosphere over a Martian year, *Icarus*, *45*, 427-446, 1981.
- Martin, L.J., Clearing the Martian air: The troubled history of dust storms, *Icarus*, *57*, 317-321, 1984.
- Moore, H.J., R.E. Hutton, R.F. Scott, C.R. Spitzer, and R.W. Shorthill, Surface materials of the Viking landing sites Mars. *J. Geophys. Res.*, *82*, 4497-4522, 1977.
- Moore, H.J. and B.M. Jakosky, Viking landing sites, remote-sensing observations and physical properties of Martian surface materials, *Icarus*, *81*, 164-184, 1989.
- Morris, R.V. and H.V. Lauer, Matrix effect for reflectivity spectra of dispersed nanophase (superparamagnetic) hematite with application to Martian spectral data, *J. Geophys. Res.*, *95*, 5101-5109, 1990.
- Morris, R.V., J.L. Gooding, H.V. Lauer and R.B. Singer, Origin of Marlike spectral and magnetic properties of a Hawaiian palagonitic soil, *J. Geophys. Res.*, *95*, 14,427-14,434, 1990.
- Mutch, T.A., R.E. Arvidson, A.B. Binder, F.O. Huck, E.C. Levinthal, S. Liebes, E.C. Morris, D. Nummedahl, J.B. Pollack, J.B. and C. Sagan, Fine particles on Mars: Observation with the Viking I Lander camera, *Science*, *194*, 87-91, 1976a.
- Mutch, T.A., A.B. Binder, F.O. Huck, E.C. Levinthal, S. Liebes, E.C. Morris, W.R. Patterson, J.B. Pollack, C. Sagan and G.R. Taylor, The surface of Mars: The view from Viking I Lander. *Science*, *193*, 791-801, 1976b.
- Mutch, T.A., et al., The surface of Mars: The view from Viking 2 Lander, *Science*, *194*, 1277-1283, 1976c.
- Palluconi, F.D. and H.H. Kieffer, Thermal inertia mapping of Mars from 60°S to 60°N, *Icarus*, *45*, 415-426, 1981.
- Pleskot, L.K. and E.D. Miner, Time variability of Martian bolometric albedo, *Icarus*, *45*, 179-201, 1981.
- Santer, R., M. Deschamps, L.V. Ksanfomaliti, and A. Dollfus L.V., Photopolarimetric analysis of the Martian atmosphere by the Soviet Mars-5 orbiter, *Astron. Astrophys.*, *150*, 217-228, 1985.
- Shorthill, R.W., R.E. Hutton, H.J. Moore, R.F. Scott and C.R. Spitzer, Physical properties of the Martian surface from the Viking 1 Lander: Preliminary results, *Science*, *193*, 805-809, 1976.
- Singer, R.B. The dark material on Mars, I, New information from reflectance spectroscopy on the extend and mode of oxydation, *Lunar Planet. Sci. XI*, 1045-1047, 1980.
- Singer, R.B., Spectral evidence for the mineralogy of high albedo soils and dust on Mars, *J. Geophys. Res.*, *87*, 10,159-10,168, 1982.
- Singer, R.B., Spectroscopic observations of Mars, *Adv. Space Res.*, *5*, 59-68, 1985.
- Singer, R.G., T.B. McCord, R.N. Clark, J.B. Adams, and R.L. Huguenin, Mars surface composition from reflectance spectroscopy: A summary", *J. Geophys. Res.*, *84*, 8415-8425, 1979.
- Singer, R.B., J.S. Miller, D.W. Well and E.S. Buss, Visible near-IR spectral images of Mars during the 1988 opposition, *Lunar Planet. Sci.*, *XXI*, 1164-1165, 1990.
- Thorpe, T.E., Viking orbiter photometric observations of the Mars phase function, July through November 1976, *J. Geophys. Res.*, *82*, 4161-4165, 1977.
- Vdovine V.V., V.S. Zhegulev, and L.V. Ksanfomaliti, Some characteristics of the soil in the equatorial zone of Mars, according to the thermal radiometry data from Mars-5. *Kosm. Issled.*, *18*, 609, 1980. (Engl. Transl., UDC 523.43:629:196.64.)
- Zimelman, J.R. and H.H. Kieffer, H.H., Thermal mapping of the northern equatorial and temperate latitudes of Mars, *J. Geophys. Res.*, *84*, 8239-8251, 1979.
- Zimelman, J.R. and L.A. Leshin, A geologic evaluation of thermal properties for the Elysium and Aeolis quadrangle of Mars, *J. Geophys. Res.*, *92*, suppl., E588-E596, 1987.
- Zurek, R.W., Martian great dust storms: An update, *Icarus*, *50*, 288-310, 1982.

M. Deschamps and A. Dollfus, Section d'Astrophysique, Observatoire de Paris, 5 place Jules Janssen, 92195-Meudon Principal Cedex, France.

J. R. Zimelman, CEPS NASM, MRC 315, Smithsonian Institution, Washington, DC 20560.

(Received December 23, 1991;  
revised June 23, 1992;  
accepted June 26, 1992.)